The Role of Droplet Collision, Evaporation and Gravitational Settling in the Modeling of Two-Phase Flows under Icing Conditions

László E. Kollár, Masoud Farzaneh*, Anatolij R. Karev
NSERC/Hydro-Québec/UQAC Industrial Chair on Atmospheric Icing of Power Network Equipment (CIGELE) and Canada Research Chair on Atmospheric Icing Engineering of Power Networks (INGIVRE) at the Université du Québec à Chicoutimi, Chicoutimi, Québec, Canada, http://www.cigele.ca

Abstract **- The effect of three important factors, droplet collision, evaporation and gravitational settling, on ice formation is investigated by applying a theoretical model of a two-phase air/dispersed water spray flow. The model simulates droplet motion in an icing wind tunnel considering these three important processes. Simulations are also carried out neglecting collision or evaporation and changing some of the ambient parameters. The set of results obtained makes it possible to determine the contribution of each of the processes examined to the modification of droplet size distribution in the wind tunnel, depending on ambient parameters.**

I. Introduction

THE process of ice accretion is greatly influenced by the size of droplets hitting the icing object and liquid water content (LWC) of the aerosol cloud near the icing object. As droplets flow through the air, their sizes undergo modification under the influence of a number of different factors, including mutual interactions within the dispersed phase, interactions between the dispersed and carrying phases, and the effect of external forces; their typical representative processes are the collision with or without coalescence, evaporation, and gravitational settling of droplets, respectively. Droplet collision tends to influence the size, trajectory and velocity of droplets thus affecting the characteristics of the flow and, thereby, the formation of ice on the icing body. The evaporation of small droplets also affects the droplet size distribution (DSD). Gravity causes the vertical deflection of droplet trajectories, thereby forming a vertical distribution in the DSD and LWC. These vertical distributions may appear nonuniform in the nature [2], however nonuniformity is more remarkable when a single spray-bar system is used to produce aerosol cloud in wind-tunnel experiments.

The process of droplet collision and the possible collision outcomes were described in detail in [6]. A composite collision outcome model was proposed, which is used in the model of the present study. A similar collision outcome model was applied in [10] for modeling binary droplet collisions in Diesel sprays. A two-dimensional model for two-phase air/dispersed water flow was also constructed in [6]. This latter model is based on the particle-source-in cell model introduced in [3] and the droplet equation presented in [8]. This two-dimensional model considers droplet collision and coalescence as well as the settling of droplets due to gravity; it excludes, however, the effect of evaporation. Simulation results obtained by applying this model predict the DSD as well as the vertical distribution of the LWC in the test section of the wind tunnel. The process of evaporation and cooling, as well as the resulting modifications in the temperature and mass of droplets were discussed in [4]. The evaporation rate and the cooling rate of a droplet were computed in accordance with [1]. The model applied in the present study is described in detail in [5], and it is basically the two-dimensional model constructed in [6], including droplet collision, gravity, and also evaporation as explained in [4]. Additionally, the present model is able to take into account a prescribed air velocity field, while constant air velocity was assumed in the simulations carried out by the former model [6].

Two-phase air/dispersed water flows created in the CIGELE atmospheric icing research wind tunnel (CAIRWT) are modeled in this research considering the following three processes: (i) droplet collision, (ii) evaporation, and (iii) gravitational settling. The sensitivity of the model presented in [5] is studied by varying the following thermodynamic parameters in the range of icing conditions: (i) initial DSD, (ii) air velocity, V_a, (iii) air temperature, T_a, and (iv) relative humidity of air, *RH*. The objective of this study is to describe the role of the three processes mentioned above in the modeling of atmospheric icing or, more precisely, to find the ranges of the four thermodynamic parameters where one or two of the three processes become dominant with regard to the evolution of DSD in the flow. A brief description of the theoretical model applied for carrying out simulations will be provided first. Simulation results will then be presented and the role of the three processes examined will be discussed. The change of median volume diameter (MVD) in the numerical modeling will be compared to previous experimental observations, and finally, conclusions will be provided.

*Chairholder

II. Two-Dimensional Model of Two-Phase Flows

The two-dimensional model constructed in [6] has been improved in [5] by considering the evaporation of droplets and a prescribed air velocity field. The construction of this model is summarized in the first part of this section, while the determination of air velocity field is discussed in the second part.

A. Model Description

The equation of motion of a droplet is given in the form [6], [8]:

$$\frac{\pi}{6}d^3\left(\rho_d+0.5\rho\right)\frac{\mathrm{d}\mathbf{v}}{\mathrm{d}t}=\frac{\pi}{6}d^3\left(\rho_d-\rho\right)\mathbf{g}+3\pi d\mu f\left(\mathbf{u}-\mathbf{v}\right), \quad (1)$$

where **v**, **u** and **g** are the droplet velocity, gas velocity, and gravity vectors, respectively, d and ρ_d are the diameter and density of the droplet, respectively, ρ and μ are the density and dynamic viscosity of the gas, respectively, while f considers the Stokes drag. The following non-dimensional parameters are defined: $\mathbf{U}=\mathbf{u}/u$, $\mathbf{V}=\mathbf{v}/u$ and $T=tu/l$, where $u=|\mathbf{u}|$, and l is the horizontal distance between the nozzles and the icing object in the tunnel. The non-dimensional equation that describes droplet motion is obtained after dividing (1) by $\left(\rho_d+0.5\rho\right)\pi d^3/6$, assuming that $\rho_d >> \rho$, and introducing the non-dimensional parameters **U**, **V** and T:

$$\frac{\mathrm{d}\mathbf{V}}{\mathrm{d}T}=\frac{l}{u^2}\mathbf{g}+\frac{18\mu l}{\rho_d d^2 u}f\left(\mathbf{U}-\mathbf{V}\right). \quad (2)$$

The parameter f varies with time, because it is a function of the Reynolds number, which depends on the droplet velocity. Therefore, (2) is integrated numerically by using the Euler scheme in a predictor-corrector mode:

$$\mathbf{V}_*=\mathbf{V}_j+\left.\frac{\mathrm{d}\mathbf{V}}{\mathrm{d}T}\right|_j\Delta T, \quad (3a)$$

$$\mathbf{V}_{j+1}=\mathbf{V}_j+\left(\left.\frac{\mathrm{d}\mathbf{V}}{\mathrm{d}T}\right|_j+\left.\frac{\mathrm{d}\mathbf{V}}{\mathrm{d}T}\right|_*\right)\frac{\Delta T}{2}, \quad (3b)$$

where ΔT is the non-dimensional time interval, the subscripts j and j+1 refer to quantities at the beginning and at the end of the time increment, respectively, while the subscript * refers to an intermediate value. After the droplet velocity at the end of the time increment is determined, the corresponding droplet position is obtained by applying the trapezoidal scheme:

$$\mathbf{X}_{j+1}=\mathbf{X}_j+\left(\mathbf{V}_j+\mathbf{V}_{j+1}\right)\frac{\Delta T}{2}, \quad (4)$$

where **X** is the dimensionless droplet position vector.

Simulation of the two-phase flow proceeds as follows. An initial DSD is provided together with the ambient parameters which serve as input data for the model. The gas velocity field is determined as will be explained in further detail in Subsection II.B. Thus, the gas velocity is a known input for many of the points where droplets may appear during the simulation. The local gas velocity at any position of the droplet in the simulation is always equal to the gas velocity calculated at the point closest to that position. Droplets are collected into parcels, because their number is too high to examine them individually. The method is based on the concept of the discrete parcel approach [9]. Each parcel contains the same number of droplets of identical size and velocity. The parcels are tracked in space and time as if they were a single droplet only, but from the collisional point of view, their size is considered larger according to the mass of droplets carried in one parcel. The position and velocity of droplet parcels are determined in each time step by applying (3) and (4), and then droplet size is reduced according to the loss of mass as well as droplet temperature is modified due to evaporation and cooling [4]. If the lost mass is greater than or equal to the mass of the droplet itself, then the droplet is evaporated and the parcel is withdrawn from further computation. Afterwards, colliding droplets are sought for. If the distance between two parcels is less than the sum of their radii, they will collide. The outcome of collisions and the sizes and velocities of post-collision droplets are determined by utilizing the composite collision outcome model [6]. If coalescence occurs then the two parcels are replaced by one parcel with larger droplets. This process is continued in the next time steps until droplets reach the icing object or simulation time finishes.

B. Air Velocity Field

The flow of water droplets in air circulating in the CAIRWT is simulated in the present study. The velocity field between the nozzles and the test section where the icing object is located should be provided as input for the simulation. Velocities are measured in the cross-sections of the nozzles and the icing object, and are computed in between by the commercial software CFX. This software is able to compute velocities in any point between the inlet and the outlet, if the geometry of the tunnel as well as the velocities in the inlet and the outlet are provided.

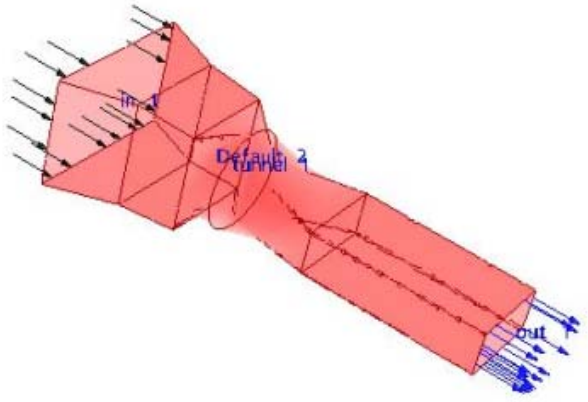

Fig. 1. The wind tunnel as it is presented in CFX

The CAIRWT is a closed-loop low-speed icing wind tunnel with a total length of about 30 m, including a 3-m long test section whose rectangular cross-section measures h_{TS} = 0.45 m in height and l_{TS} = 0.9 m in width. The icing body is placed in the middle of the test section, which is 4.4 m downstream from the spray-bar. The cross-section of the tunnel at the spray bar is also rectangular with a height of 1.12

m and width of 1.7 m. The tunnel becomes circular 1.5 m downstream from the spray bar with diameter of 1 m. The cross-section contracts further in the next 1.1 m reaching the final rectangular cross-section of the size of the test section. A draft of the wind tunnel as it is presented in CFX can be seen in Fig. 1. Since the present model of the two-phase flow is two-dimensional, only the vertical plane in the middle of the tunnel is considered.

III. Results of Sensitivity Tests

Simulation results are presented in this section. One of the ambient parameters is varied, while other parameters are maintained constant in each subsection. Then, the ranges of the ambient parameters where the effects of droplet collision, evaporation and gravity are important with regard to the evolution of DSD in the wind tunnel are determined.

The flow in the wind tunnel was simulated between the following two locations: 50 cm downstream from the nozzle-equipped spray bar where the disintegration of liquid jet had been completed, and the test section where the icing object is located. The output of simulations is the DSD at the position of the icing object in the test section. This DSD is obtained by considering all or some of the droplets occurring in the last 10 % of the tunnel where the flow is simulated. Some of the results presented are related to the entire height of the test section, implying that all the droplets will be taken into account. Other DSDs are obtained by considering droplets which appear only in the vicinity of the centerline. The location of these droplets is defined by the vertical length where droplets occur at the beginning of the simulation. This length may easily be calculated from the diameter of the nozzle outlet, d_0; the spray angle of the nozzles, α, (both data provided by the manufacturer); and, the distance from the nozzle outlet, l_0, which is selected at 50 cm as mentioned earlier in this paragraph. The term *vicinity of the centerline* refers to this calculated range in what follows, and the length of this range for the spray angle $\alpha = 15^\circ$ is obtained by applying the formula:

$$h_0 = d_0 + 2l_0 \tan\frac{\alpha}{2} = 1.2\cdot 10^{-3} + 2\cdot 0.5\cdot \tan\frac{15^\circ}{2} = 0.133\ \text{m}. \quad (5)$$

The result obtained using this formula indicates the range between 6.65 cm above and 6.65 cm below the centerline.

A. Combined Effect of Air Velocity and Initial DSD

A simplified version of the model was used in the first set of simulations. Droplet collision and evaporation were neglected, and the air velocity as well as the initial DSD was varied in order to find the domains of these parameters where gravity influences the vertical uniformity of DSD.

Simulations were carried out for four different air velocities: 5 m/s, 10 m/s, 20 m/s, and 30 m/s, while two different DSDs were used as input data. They represent the DSDs obtained in earlier experiments [7] for two different combinations of the nozzle-dynamic parameters, i.e. the gauge pressure in the water line, p_L, and the gauge pressure in the air line, p_A. The first DSD is obtained for p_L = 345 kPa, p_A = 276 kPa, while the second one is obtained for p_L = 449 kPa, p_A = 173 kPa; the corresponding MVDs are 36.8 μm and 61.8 μm, respectively. It should be noted that these values are slightly different from those presented in [7], in view of the fact that the number of parcels with large-diameter droplets is low, and that the contribution of these droplets to the total mass of droplets in the aerosol cloud is significant. Thus, the round-off of the number of parcels to an integer value may result in a slight discrepancy between the MVDs of the measured and simulated DSD. The air temperature was -20 °C, while the relative humidity did not play a role in this set of simulations, since evaporation was not considered.

Fig. 2 shows the ratio of MVD at the icing object in the test section in the vicinity of the centerline, $D_{0.5,\text{TSc}}$, to that at the spray bar, $D_{0.5,\text{SB}}$, for different air velocities and initial DSDs. The MVD decreases to a considerable extent for low air velocities (5-10 m/s), but it is not modified for velocities greater than 20 m/s. A further important result is that the extent the MVD decreases to is less for sprays with smaller droplets than for sprays with larger droplets. The observations after this set of simulations reveal that gravity causes vertical separation of droplets of different sizes, and thereby, affects the DSD in the vicinity of the centerline where the icing object is located for low air velocities. Furthermore, this effect is more significant for aerosol clouds with larger droplets.

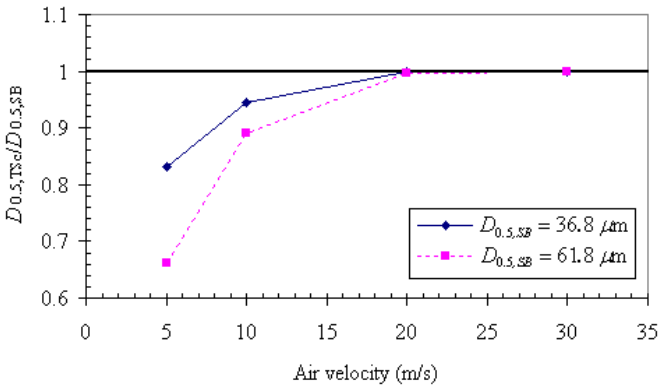

Fig. 2: The ratio of MVD at the icing object in the vicinity of the centerline to MVD at the spray-bar as a function of air velocity

B. Air Velocity

The DSD with MVD of 36.8 μm was used in further simulations, and droplet collision or evaporation or both of them were considered. The air temperature and the relative humidity were -20 °C and 0.7, respectively, in these simulations. The comparison of Fig. 3(a) and Fig. 3(b) confirms the consequences of the previous subsection. Fig. 3(a) presents the ratio of MVD at the icing object in the test section, $D_{0.5,\text{TS}}$, to that at the spray bar, $D_{0.5,\text{SB}}$, while Fig. 3(b) shows the ratio $D_{0.5,\text{TSc}} / D_{0.5,\text{SB}}$. If only evaporation is considered, the MVDs obtained in the test section for low air velocities (5 – 10 m/s) are almost the same as those for higher

velocities (20 – 30 m/s) as shown in Fig. 3(a). If collision alone, or both collision and evaporation are considered, then the MVDs obtained in the test section for low air velocities are greater than those in the case of higher velocities. However, the MVD in the vicinity of the centerline at the test section increase with air velocity in a range of velocity less than 20 m/s as may be seen in Fig. 3(b). The reason for this result is that gravity separates droplets of different sizes for air velocities less than 20 m/s. Small droplets always stay in the vicinity of the centerline, while large droplets tend to approach the bottom of the tunnel.

Figs 3(a) and 3(b) also emphasize the effect of collision on droplet size. The MVD is always greater when collision is considered in the model compared to the simulations when collision is neglected. The degree of this difference is usually around 20-25 %, but it may even reach 70 % for low air velocities. This fact may be explained by the higher vertical component of velocity of large droplets due to gravity, which leads to greater number of collisions. The difference between the results obtained with and without considering evaporation, however, is not significant.

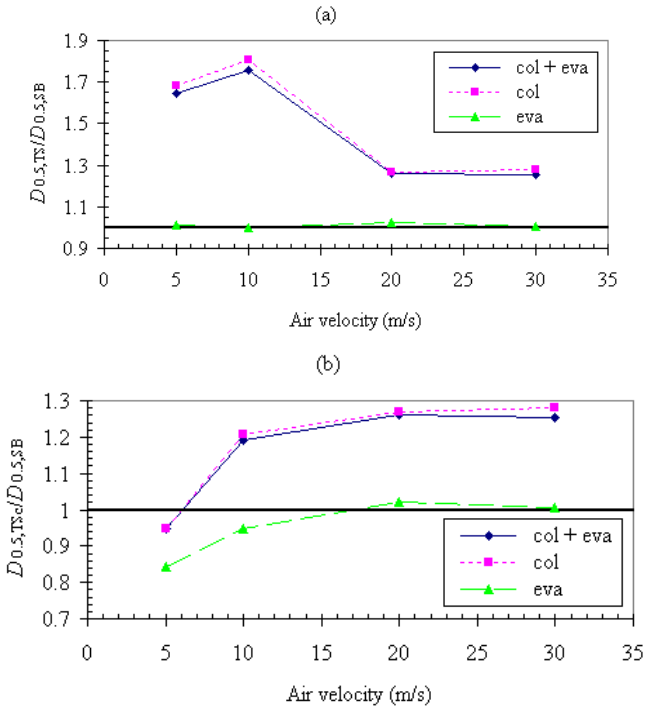

Fig. 3. (a) The ratio of MVD at the icing object in the entire height of the test section to that at the spray bar as a function of air velocity; (b) the ratio of MVD at the icing object in the vicinity of the centerline to that at the spray bar as a function of air velocity. Abbreviations: col: collision, eva: evaporation

The change in the DSD during droplets pass the tunnel can be followed in Fig. 4. Since evaporation did not modify droplet size significantly under the conditions examined, results are shown for the case when collision only is considered. Air velocity was chosen to be 5 m/s in order to also demonstrate the effect of gravity. This figure clearly shows that the ratio of small droplets (d < 30 μm) decreases, while the ratio of middle-size and large droplets (d > 30 μm) increases during simulation. With regard to DSD in the vicinity of the centerline, the ratio of small droplets (d < 30 μm) decreases, and the ratio of middle-size droplets (30 μm < d < 70 μm) increases slightly, but the largest droplets (d > 70 μm) approach the bottom of the tunnel due to gravity. Thus, these are not part of the DSD obtained in the vicinity of the centerline.

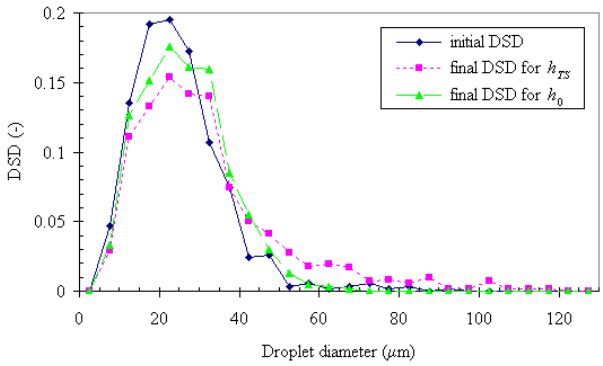

Fig. 4. DSDs for 5 m/s when droplet collision is considered and evaporation is neglected

C. Air Temperature

Air temperature was varied between -20 °C and 0 °C in the next set of simulations, with DSD with 36.8 μm MVD, 10 m/s air velocity, and 0.7 relative humidity. Although the relative humidity is usually greater than 0.7 under icing conditions, this value was chosen for this set of simulations because it makes the effect of evaporation easier to demonstrate. The effect of evaporation is more significant for lower values of relative humidity as will be shown in Subsection III.D. Simulations were carried out with droplet collision or evaporation or both of them taken into account.

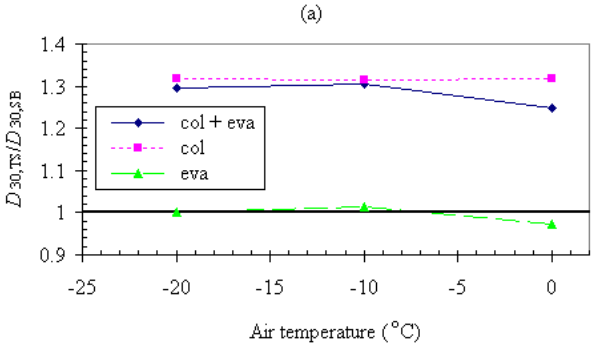

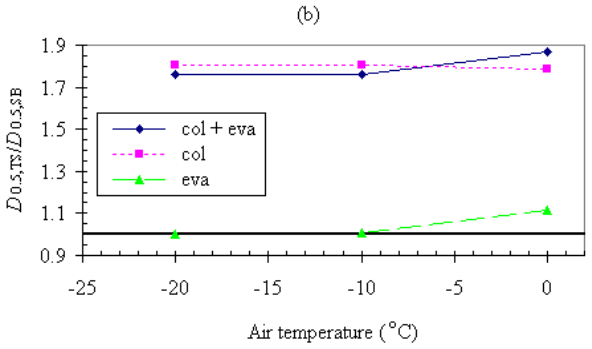

Fig. 5. (a) The ratio of MMD at the icing object in the entire height of the test section to that at the spray bar as a function of air temperature; (b) the ratio of MVD at the icing object in the entire height of the test section to that at the spray bar as a function of air temperature. Abbreviations are as in Fig. 3

The ratio of mass mean diameter (MMD) in the test section, $D_{30,TS}$, to that at the spray bar, $D_{30,SB}$, is shown in Fig. 5(a), while the ratio of MVD in the test section, $D_{0.5,TS}$, to that at the spray bar, $D_{0.5,SB}$, can be seen in Fig. 5(b), for three different air temperatures, -20 °C, -10 °C and 0 °C. Both the MMD and the MVD are approximately constant if collision is considered, but evaporation is neglected. If evaporation is also considered, then an interesting phenomenon can be observed. The MMD decreases if air temperature increases, while the MVD increases with it. A possible explanation of this result is as follows. The effect of evaporation is negligible for low temperatures, but its effect becomes important as temperature approaches 0 °C. Also, the influence of evaporation is more considerable on small droplets. The smallest droplets are evaporated completely, while the size of the middle-size ones decreases significantly. However, the size of the largest droplets remains almost constant. The MMD decreases due to the general decrease in droplet size. On the other hand, the number of small droplets decreases and the number and size of large droplets do not change significantly. Since the contribution of large droplets to the MVD becomes more significant, the MVD increases.

Neither the MMD nor the MVD is modified by more than 10 % even at the highest temperature, 0 °C, according to Figs 5(a) and 5(b). The importance of evaporation with increasing temperature, however, can clearly be seen in Table I where the ratio of evaporated droplets, N_{eva} / N_0, is shown for different values of air temperature, T_a. It should be noted that the influence of evaporation on droplet size would appear more significant if longer distances were simulated, and thereby, simulation time was increased. Furthermore, as discussed in [4], evaporation may influence droplet size to a great extent under certain conditions, such as for air temperatures higher than those in the present simulations, or in the presence of aerosol clouds with droplets smaller than those modeled in this paper.

TABLE I
RATIO OF EVAPORATED DROPLETS FOR DIFFERENT VALUES OF AIR TEMPERATURE. ABBREVIATIONS ARE AS IN FIG. 3

T_a (°C)	N_{eva} / N_0 (%) col + eva	N_{eva} / N_0 (%) eva
-20	0	0
-10	2.1	3.7
0	3.1	4.6

D. Relative Humidity of Air

The relative humidity of air was varied between 0.7 and 0.9 in the last set of simulations, with DSD with 36.8 μm MVD, 10 m/s air velocity, and 0 °C air temperature. Although this temperature is the upper limit of icing conditions, it was chosen for this set of simulations, because it allows for a clearer illustration of the effect of evaporation. The effect of evaporation is more significant for higher air temperatures according to the previous subsection. Simulations were carried out with droplet collision or evaporation or both of them taken into account.

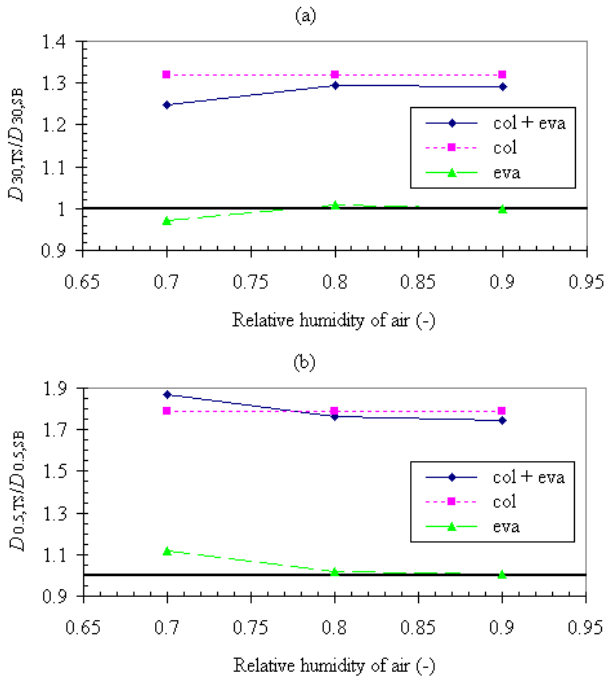

Fig. 6. (a) The ratio of MMD at the icing object in the entire height of the test section to that at the spray bar as a function of relative humidity of air; (b) the ratio of MVD at the icing object in the entire height of the test section to that at the spray bar as a function of relative humidity of air. Abbreviations are as in Fig. 3

The ratios, $D_{30,TS} / D_{30,SB}$ and $D_{0.5,TS} / D_{0.5,SB}$, are shown in Figs 6(a) and 6(b), respectively, for three different values of relative humidity, 0.7, 0.8 and 0.9. A tendency very similar to that observed in Figs 5(a) and 5(b) can be seen in these diagrams. Neither the MMD nor the MVD changes with relative humidity if only droplet collision is allowed; however, evaporation has the same effect as was observed for varying air temperatures, albeit in the opposite direction. The MMD decreases with relative humidity as the effect of evaporation becomes more significant; the MVD increases, however, at the same time. The argument of the previous subsection that explained the reverse modification of MMD and MVD due to the change of air temperature may also apply to explain the

similar effect of relative humidity.

TABLE II
RATIO OF EVAPORATED DROPLETS FOR DIFFERENT VALUES OF RELATIVE HUMIDITY OF AIR. ABBREVIATIONS ARE AS IN FIG. 3

RH (-)	N_{eva} / N_0 (%) col + eva	N_{eva} / N_0 (%) eva
0.7	3.1	4.6
0.8	2.4	3.9
0.9	0	0

Similarly to the results presented for different air temperatures, the MMD and the MVD do not change by more than 10 % for any values of relative humidity in the range examined and during the simulation time considered. Table II confirms, however, that the influence of evaporation becomes more considerable as relative humidity, *RH*, decreases.

IV. COMPARISON OF SIMULATION AND FORMER EXPERIMENTAL RESULTS

Measurements of DSD at the test section were reported in [4]. The DSD was measured by applying the collargol slide impact method. A small slide coated by collargol is placed inside a horizontal cylinder. This cylinder is covered with an aluminum pipe which has a rectangular opening for exposing the slide to the flow. Droplets are captured on the slide, and their diameters are measured by a Scienscope microscope. Experiments were carried out for two combinations of nozzle-dynamic parameters only. One of them (p_L = 365 kPa, p_A = 276 kPa) was almost the same as the combination (p_L = 345 kPa, p_A = 276 kPa) used in most of the numerical modeling presented in this paper. The MVDs obtained for these conditions are compared in Table III. The values of the other parameters in the experiment were: $T_a = 20\,^{\circ}\mathrm{C}$, RH = 0.8, and V_a = 10 m/s, while the same parameters in the simulation with closest conditions are: $T_a = 0\,^{\circ}\mathrm{C}$, RH = 0.8, and V_a = 10 m/s.

Table III shows measured and computed MVDs at the spray-bar (column II) and in the vicinity of the centerline at the test section (column III), moreover, it shows the ratio of increase of the MVD (column IV). It can be seen that the difference between this ratio in the measurement and the one in the simulation is only 3%. It should be clear, however, that this comparison alone is not sufficient to validate the simulation results. Therefore, the next step in future works will be to carry out a set of experiments in the test section and compare them to simulation results.

TABLE III
COMPARISON OF SIMULATION AND EXPERIMENTAL RESULTS

p_L / p_A (kPa)	$D_{0.5,SB}$ (μm)	$D_{0.5,TS}$ (μm)	$D_{0.5,TS} / D_{0.5,SB}$
365/276 (measured in [4])	36.5	41.8	1.15
345/276 (computed in the present study)	36.8	43.6	1.18

V. CONCLUSIONS

Two-phase air/dispersed water flows in an icing wind tunnel with a single spray-bar system have been simulated. Droplet collision, evaporation and gravitational settling were considered in the model, and their effects on the MVD and DSD were examined when initial DSD, air velocity, air temperature and relative humidity of air were varied.

1. Among the three processes investigated, droplet collision leads to modification in droplet size to the greatest extent under icing conditions. The MVD increases by around 20-25 % due to collision; it may increase, however, by up to 70 % for low air velocities (5 – 10 m/s). Changing air temperature or air relative humidity does not affect the influence of collision.
2. Gravity causes vertical separation of droplets of different size. Larger droplets settle down more quickly than smaller ones, with the larger ones tending to approach the bottom of the tunnel, and the smaller ones stay in the middle. This effect occurs at low air velocities. It is negligible for velocities greater than 20 m/s, but it is amplified if the MVD of the aerosol cloud increases.
3. The effect of evaporation becomes considerable if air temperature approaches the upper limit of icing conditions (around $0\,^{\circ}\mathrm{C}$), or if relative humidity of air approaches its lower limit (around 0.7). The MMD decreases, while the MVD increases slightly when approaching the range of temperature and relative humidity where evaporation is important.

VI. ACKNOWLEDGMENT

This research was carried out within the framework of the NSERC/Hydro-Quebec Industrial Chair on Atmospheric Icing of Power Network Equipment (CIGELE) and the Canada Research Chair on Atmospheric Icing Engineering of Power Network (INGIVRE) at the Université du Québec à Chicoutimi (UQAC). The authors would like to thank all the sponsors of the CIGELE for their financial support. We are also grateful to Z. Peter for his valuable help in CFX computations.

VII. REFERENCES

[1] K. V. K. Beard, "A Wind Tunnel Investigation of the Terminal Velocities, Collection Kernels and Ventilation Coefficients of Water Drops Freely Falling in Air," PhD thesis, University of California, Los Angeles, 1970.

[2] S. G. Cober, J. W. Strapp, and G. A. Isaac, "An Example of Supercooled Drizzle Drops Formed through a Collision-Coalescence Process," *Journal of Applied Meteorology*, vol. 35, pp. 2250-2260, 1996.

[3] C. T. Crowe, M. P. Sharma, and D. E. Stock, "The Particle-Source-In Cell (PSI-CELL) Model for Gas-Droplet Flows," *Journal of Fluids Engineering*, pp. 325-332, 1977.

[4] A. R. Karev and M. Farzaneh, "Evolution of Droplet Size Distribution in an Icing Wind Tunnel," in *Proc. of the 10th Int. Workshop on Atmospheric Icing of Structures*, Brno, Czech Republic, 2002, paper 7.3.

[5] A. R. Karev, M. Farzaneh, and L. E. Kollar, "Evolution of Droplet Size Distribution in an Icing Wind Tunnel: Laminar Air Flow Assumption," to be submitted to *Int. J. Multiphase Flow*, 2005.

[6] L. E. Kollar, M. Farzaneh, and A. R. Karev, "Modeling Droplet Collision and Coalescence in an Icing Wind Tunnel and the Influence of these Processes on Droplet Size Distribution," *Int. J. of Multiphase Flow*, vol. 31, pp. 69-92, 2005.

[7] L. E. Kollar, M. Farzaneh, and A. R. Karev, "Modeling Droplet-Size Distribution at the Nozzle Outlet an Icing Wind Tunnel," *Atomization and Sprays*, submitted in 2004.

[8] M. R. Maxey and J. J. Riley, "Equation of motion for a small rigid sphere in a nonuniform flow," *Physics of Fluids*, vol. 26(4), pp. 883-889, 1983.

[9] P. O'Rourke and F. Bracco, "Modeling of drop interactions in thick sprays and a comparison with experiments," *Proceedings of the Institution of Mechanical Engineers*, vol. 9, pp. 101-116, 1980.

[10] S. L. Post and J. Abraham, "Modeling the outcome of drop-drop collisions in Diesel sprays," *Int. J. of Multiphase Flow*, vol. 28, pp. 997-1019, 2002.

Corresponding author: László E. Kollár, Postdoctoral Fellow, NSERC/Hydro-Québec/UQAC Industrial Chair on Atmospheric Icing of Power Network Equipment (CIGELE) and Canada Research Chair on Engineering of Power Network Atmospheric Icing (INGIVRE), Université du Québec à Chicoutimi, 555, Boulevard de l'Université, Chicoutimi, Québec, Canada, G7H 2B1, E-mail: laszlo_kollar@uqac.ca